DOI: 10.1002/ecv.70208

REPORT



Check for updates

Hidden decay of live trees in a tropical rain forest

Javier O. Ballesteros² | César A. Barrios-Rodríguez² | Ernesto Bonadies² | Marjorie L. Cedeño-Sánchez | Nohely J. Fossatti-Caballero | José Moisés Pérez-Suñiga² | Mariam M. Trejos-Rodríguez² | Stephen P. Hubbell^{2,5}

Correspondence

Gregory S. Gilbert Email: ggilbert@ucsc.edu

Funding information

Division of Environmental Biology, Grant/Award Numbers: DEB-00753102, DEB-0129874, DEB-0346488, DEB-0425651, DEB-0640386, DEB-1136626, DEB-1437419, DEB-7922197, DEB-8206992, DEB-8605042, DEB-8906869, DEB-9100058, DEB-9221033, DEB-9405933, DEB-9615226, DEB-9909347; Small World Institute Fund; John D. and Catherine T. MacArthur Foundation: Andrew W. Mellon Foundation; Smithsonian Tropical Research Institute; Forest Global

Handling Editor: Joseph B. Yavitt

Earth Observatory (ForestGEO)

Abstract

The trunks of forest trees store massive amounts of carbon, but fungi actively and invisibly decay wood inside even seemingly healthy trees. Wood-decay fungi are responsible for the loss of stored carbon in living trees, and they make trees susceptible to snapping and uprooting in storms. We used sonic tomography to measure the prevalence and severity of decay in 1744 live trees (≥20 cm diameter) of 171 species on the 50-ha Forest Dynamics Plot on Barro Colorado Island, Panama. A median of <2% of the cross-sectional trunk area showed decay, but 15% of trees had >20% decay. Twenty percent of the combined basal area showed decay, representing a loss of approximately 1% of aboveground biomass. Larger trees more often showed internal decay, with one quarter of trees showing decay before reaching canopy height. Decay severity varied by species; 23% of species showed <2% decay while 9% of species lost over half their basal area. Rare species were more affected than locally abundant species, and species with traits associated with a fast life history were more susceptible to decay. These results suggest that hidden wood decay affects a large proportion of living tropical forest trees.

KEYWORDS

Barro Colorado Island, carbon storage, density dependence, lignolytic fungi, Panama, plant disease, tomography, tropical forest, wood decay

This is an open access article under the terms of the Creative Commons Attribution License, which permits use, distribution and reproduction in any medium, provided the original work is properly cited.

© 2025 The Author(s). Ecology published by Wiley Periodicals LLC on behalf of The Ecological Society of America.

¹Department of Environmental Studies, University of California Santa Cruz, Santa Cruz, California, USA

²Smithsonian Tropical Research Institute, Panama, Republic of Panama

³Department of Biological Sciences and Museum of Natural Science, Louisiana State University, Baton Rouge, Louisiana, USA

⁴Department of Environmental Health Science, University of Georgia, Athens, Georgia, USA

⁵Department of Ecology and Evolutionary Biology, University of California, Los Angeles, Los Angeles, California, USA

INTRODUCTION

Tree trunks play central roles in our understanding of forest ecology because forest diversity, spatial structure, and dynamics are often studied by mapping and measuring them (Blundo et al., 2021; Davies et al., 2021). Trees capture carbon in radial growth through the production of cellulose, hemicellulose, and lignin (Cabon et al., 2022). However, tree trunks are susceptible to attack by wood-decay fungi, leading to reduced growth (Hellgren & Stenlid, 1995), tree mortality, and forest disturbance (Hansen & Goheen, 2000), as well as reduced carbon storage (Russell et al., 2015). Here, we uncover the scale and patterns of wood decay hidden inside living trees in a tropical forest and explore the implications of wood decay for both carbon sequestration and the maintenance of tree diversity.

Mature forest trees are strongly affected by wood-decay fungi that act as root-rot, butt-rot, and heart-rot pathogens, attacking the woody biomass held in trunks and root systems (Worrall et al., 2005). Whereas some wood-decay fungi can kill trees outright (Aguadé et al., 2015; Dobbertin et al., 2001), many root-, butt-, and heart-rot pathogens contribute to mortality by making their tree hosts more susceptible to snapping and uprooting by degrading structural woody tissues (Kodrík & Kodrík, 2002). Because wood-decay fungi act slowly, heart rot is often more common in large-diameter trees (Kõrkjas et al., 2021). Trade-offs in growth and defense mean that tree species with fast life histories are expected to suffer greater impacts from natural enemies than species with slow life histories (Chave et al., 2009). Unfortunately, most work on the impact of diseases on mature trees has focused on a few commercially important species (Bruck, 1989; Worrall et al., 2005), with remarkably little work on their impact on the physical structure or mortality of trees outside of managed forests. And, although studies using harvested wood show that high density or high terpene content reduces susceptibility to decay fungi (Kahl et al., 2017), we lack studies of how host life history traits (Chave et al., 2009) moderate the effects of fungal pathogens in more diverse forests.

Fungi also play a role in forest diversity, and the impact of conspecific negative density-dependent disease of juvenile trees is thought to be an important mechanism for the maintenance of tropical tree diversity (Comita & Stump, 2020; Johnson et al., 2012). Under this hypothesis, host-specialized pathogens respond positively to the density of their hosts so that locally abundant host species should suffer greater disease impacts than rare ones. Most studies of disease in wild communities have focused on fast-acting pathogens with polycyclic life cycles that attack juvenile plants and that spread readily among nearby

hosts (Augspurger & Kelly, 1984; Balmelli et al., 2013). However, decay pathogens of mature tree trunks have life histories that differ significantly from pathogens that attack juveniles (Delaye et al., 2013), with potentially different downstream effects on the diversity of mature trees. Wood-decay pathogens are mostly slow-growing basidiomycete fungi with reproduction delayed for decades after infection; they often spread among individuals with intertwined root systems rather than by air-borne spores; and they can thrive on dead woody material (Chung et al., 2015; Hansen & Goheen, 2000; Page et al., 2020). These traits may decouple plant and pathogen population dynamics, limiting density responsiveness.

Forest trees are also dynamic carbon sinks, capturing net global 1.1–1.4 Pg C year⁻¹ (Martin et al., 2021). Wood in dead-standing and fallen trees on average contains 48.5% carbon, representing 8% of the total global forest C pool (Martin et al., 2021). Large, living trees, however, dominate carbon storage in forests (Lutz et al., 2018), and allometric calculations of the amount carbon stocks held in trees assume that tree trunks are solid wood (Chave et al., 2005; Gonzalez-Akre et al., 2021). Yet, wood-decay fungi reduce wood density inside living trees by breaking down the cellulose, hemicellulose, and (in some cases) lignin that comprise the major components of wood (Fukasawa, 2021), making accurate measures of the extent of heart rot in living trees essential to reliable estimates of forest carbon stocks (Nogueira et al., 2006). Most estimates of such loss come from felled trees of a few commercially important species and suggest that up to 80% of individuals suffer from wood decay, with 20% of trees having decay hollows and a loss of up to 7% of merchantable wood volume (Barry et al., 2004; Basham, 1973; Rojo & Paquit, 2018; Sudin et al., 1992; Sundararaj et al., 2023).

Here, we use noninvasive tomography approaches to evaluate the amount of heart rot in live individuals of all large tree species in a moist tropical forest. We estimate the overall prevalence and severity of decay in standing trunks, examine the relationship between tree size and decay severity, and evaluate density dependence within and across host species. We also test whether life history traits are indicators of variation in internal decay among tree species and whether internal decay is correlated with readily visible signs of fungi or arthropod associates that may facilitate detection of decay.

METHODS

Site and tree species data

We conducted the study on the mapped 50-ha Forest Dynamics Plot (FDP) (Condit et al., 2019a, 2019b;

ECOLOGY 3 of 9

Hubbell et al., 1999) on Barro Colorado Island (BCI) in the Republic of Panama during February 2012 to April 2014. The BCI FDP is managed by the Smithsonian Tropical Research Institute and located in a tropical moist deciduous forest (latitude: 9.1543, longitude: –79.8461) with a mean elevation of 120 m, 2580 mm of average annual precipitation, and an average annual cumulative moisture deficit of –514 mm. We used tree location data and 2010 diameter at standard height (DSH; measured at 1.3 m) of trees provided through ForestGEO (https://forestgeo.si.edu). We updated tree species taxonomy to conform with World Flora Online (WFO) plant list (https://www.worldfloraonline.org/, 28 July 2024) using R package TNRS (Boyle et al., 2013) (Appendix S1: Table S1).

Selection of trees to scan

We selected the sample of trees to scan by constraining the total list of trees in the FDP to the 7642 living trees larger than 20-cm DSH in the 2010 plot census, because this is the minimum size needed for reliable tomography (Gilbert et al., 2016). We then designed a sampling scheme to ensure that we scanned all species in the FDP from the rarest to the most common. We selected the 20-m × 20-m quadrats that contained any individual of a rare species (those with ≤ 10 stems on the FDP). On visiting each of those 302 quadrats (24% of the plot area), we used sonic tomography (described below) to measure internal decay in each tree. When trees had multiple large stems, we scanned the largest stem, and we excluded any individual found dead. In this way, we scanned all living stems of the 91 rare species, along with a subsample of stems of the remaining species (Appendix S1: Figure S1).

Sonic tomography

To measure the degree of decay in living trees, we used the Picus 3 sonic tomograph (Argus Electronic) to scan a cross section of each tree at 1 m above ground level, following methods we previously validated (Gilbert et al., 2016). We scanned trees at 1 m above ground level rather than lower because we were interested in collecting both sonic tomography data (this paper) and electrical impedance tomography (data not shown), and the impedance measurements are sensitive to being too close to branching structures like roots (PiCUS, 2015). For each scan, we used the open-access ImageJ software (National Institutes of Health, Bethesda, Maryland, USA; http://imagej.nih.gov) to calculate the total cross-sectional area of the trunk and the proportion of the area showing moderate (greenish hues)

or severe (blue to magenta hues) decay (Gilbert et al., 2016). During the scanning procedure, we also recorded the presence of macroscopic fungal reproductive structures on the tree, and nests or trails of ants (*Azteca trigona*) or termites (*Nasutitermes corniger*) on each tree.

We confirmed internal wood decay by drilling into trunks at positions that tomography identified as being decayed. Specifically, we collected cores by first removing a small section of bark with a knife (sterilized with 0.525% sodium hypochlorite and 70% ethanol) from the areas closest to presumed decay; we sprayed the surface of the exposed wood and then sprayed it with 70% ethanol. Then, we collected a single core from each tree using a sterile 5-mm spade drill bit and an electric drill until we detected decay by visually examining the drill shavings, up to a maximum depth of 15 cm. Between uses, we carefully cleaned and autoclaved all drill bits after wrapping them loosely in aluminum foil. To prevent unnecessary damage to the trees, we did not take cores from any trees where tomography indicated there was zero or minimal decay.

Analysis

We performed all analyses using the R statistical platform (v 4.3.1). The full dataset is available on Dryad (https://doi.org/10.5061/dryad.kprr4xhfx).

To evaluate whether there were underlying spatial patterns in decay prevalence or severity, we examined a generalized additive model (GAM, using mgcv package) of prevalence (with decay threshold of 5%) or severity as a function of DSH, with stem location (in meters east and north of the southwest corner of the plot) as a smoothing function. There was no significant effect of spatial location in either model (for prevalence: edf = 9.99, F = 1.43, p = 0.128, df = 13.12; model deviance explained = 13.5%, adjusted $R^2 = 0.129$, GCV = 0.182; n = 1744; for severity: edf = 4.369, F = 1.183, p = 0.33, df = 5.75; model deviance explained = 20.2%, adjusted $R^2 = 0.199$, GCV = 0.029; n = 1744), and we did not include spatial location in further analyses.

We conducted logistic regressions (glm, family binomial, logit link) to evaluate the likelihood of heart rot as a function of tree size and species abundance on the plot. Species abundance estimates only included stems with DSH \geq 20 cm because heart rot is much less likely to affect (or spread from) small individuals. We evaluated the presence of heart rot at different severity thresholds: 2%, 5%, 10%, and 20% of the cross-sectional area, and because there was a significant interaction between abundance and DSH, we included that term in analyses.

We conducted similar logistic regressions to examine whether the likelihood of heart rot reflected tree life history traits commonly associated with fast life histories (little investment in defense in favor of rapid growth and early reproduction) or slow life histories (longer life spans and greater investment in defenses), and we derived these parameters from wood economics spectrum data compiled for BCI tree species by Wright et al. (2010). We focused on three traits: relative growth rate (of trees larger than 100 mm DSH); mortality rates of trees larger than 10 or 100 mm, for which larger values are associated with a fast life history strategy; and wood density, for which larger values are associated with a slow strategy.

We used a tobit regression (vglm function in the VGAM package) to evaluate the effects of tree size and species abundance on the plot relative to the severity of decay, because estimates of decay are not possible below 0%, inflating the number of values at 0% decay. The smallest measured proportion of decay was 0.00014; so, we then added 0.0001 to all decay estimates and multiplied that sum by 100. We calculated the base-10 logarithm of that value to improve normality in the (noninflated) decay estimates. The tobit regression included a lower bound of $\log_{10}((0.00014 + 0.0001) \times 100)$. Because there was no significant interaction between abundance and DSH, we used a simple additive model.

To assess whether the presence of visible rot, fungal reproductive structures, and ant or termite colonies was associated with the severity of decay, we conducted logistic regressions (glm, family binomial, logit link) to evaluate the likelihood of the presence of each of those associates as a function of the cross-sectional area showing decay and tree diameter in an additive model.

RESULTS

Broad patterns of decay across all species

Internal wood decay was widespread across the 1744 scanned trees of 172 species (Figure 1A; Appendix S1: Figure S1 and Table S1). Scanned trees ranged in diameter from 20 to 131 cm (median 29.7 cm; mean 35.7 ± 17.2 cm). Sonic tomography revealed that decay was present in 90.7% of stems, and the median cross-sectional area lost to decay was 1.87% ($10.11\% \pm 19.04\%$; mean \pm SD). Among scanned trees, 34.17% of trunks had <1% decay, 51.72% had <2%, and 15.88% had >20% decay (Figure 1A).

Larger trees were more likely to suffer internal wood decay, regardless of the threshold percent decay used

(Figure 1B). Although the median diameter of scanned trees was 297 mm, it was not until 366 mm (the 84% quantile of trunk diameters) at which half of all trunks showed signs of wood decay (at a 2% decay severity threshold). At greater severities, the midpoint was not reached until 562 mm (5% threshold), 647 mm (10%), or 962 mm (50%).

The total cross-sectional area of all 1744 scanned trees was 359.52 m² and total area with decay was 86.63 m², which means that 19.99% of the cross-sectional area showed wood decay. Similarly, 11.22% of the total cross-sectional area suffered "severe" decay.

Estimating loss of aboveground biomass to decay is limited by an absence of two critical pieces of information: the height of the decay column within trees and the proportion of biomass lost in areas undergoing decay. Using extreme upper-bound assumptions, including 100% biomass loss in decayed areas, we estimate that the maximum possible loss of aboveground biomass for scanned trees would be 10% (Appendix S2). Literature estimates of decay-column height allow more realistic estimates of upper-bound losses to be in the range of 0.92%-2.58%. However, much of the decay column is not hollow, with something less than 100% biomass loss. Based on these considerations, a rough estimate of the total aboveground biomass of living trees that is lost to internal decay is ~1% (Appendix S2).

Variation across species

Species varied in prevalence and severity of decay (Figure 1C). About a quarter of all species had <2% lost to decay, nearly half suffered >10% decay, and 14 species (9% of scanned species) lost $\geq 50\%$ of their cross-sectional area to decay. The severity and prevalence of decay were strongly correlated (Appendix S3: Figure S1), indicating that species more likely to show any decay were also more likely to exhibit severe decay.

Rare species were more often decayed than common species, at all thresholds of decay severity (Figure 1D). The effect of species abundance on decay severity was similar to that for decay prevalence, with no significant interaction between abundance and trunk diameter. Larger trunks and rarer species were more likely to have severe decay (Appendix S3: Figure S2).

We found no local effects of conspecific density on decay. Analysis of effects of conspecific density within $20\text{-m} \times 20\text{-m}$ quadrats or based on distance to nearest conspecific neighbors provided no findings different from those based on overall species abundance (Appendix S4).

ECOLOGY 5 of 9

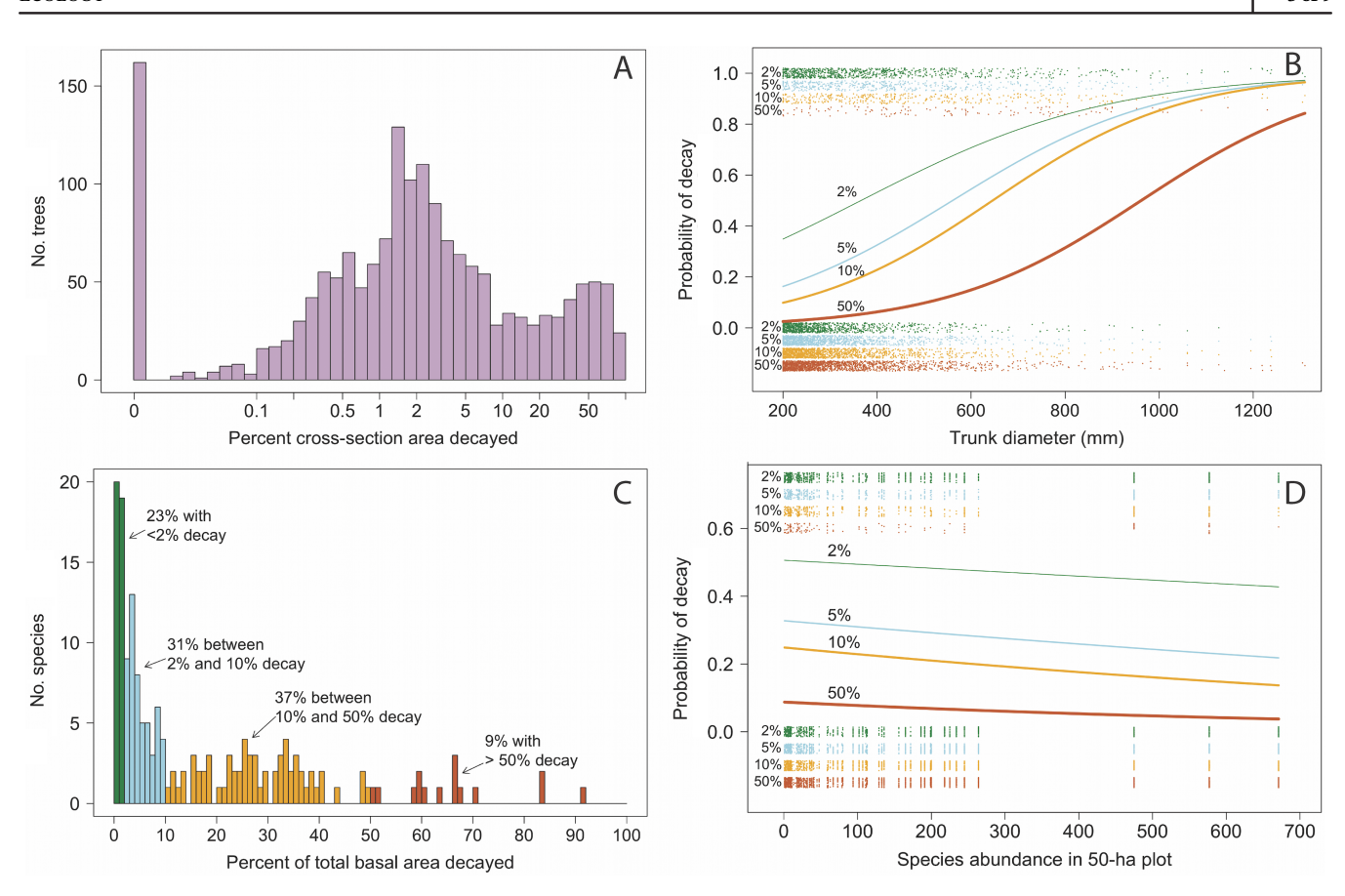


FIGURE 1 (A) Percentage of cross-sectional area estimated by tomography that showed decay. Decay area is on a log₁₀(percent decay + 0.01) scale to reveal the multimodal distribution in greater detail. Because negative values of decay are not possible, there is an inflation of zero values, illustrated by the 162 trees at 0% decay. (B) Probability of wood decay across 1744 trunks of 172 tree species. Logistic regressions shown for decay thresholds of 2%, 5%, 10%, and 50% of cross-sectional basal area decayed. Regression formulas are logit(decay2%) = $-1.37852 + 0.00377 \times \text{diameter}$ (slope SE = 0.00036, z = 10.37, p < 0.001; residual deviance of 2278.6 on 1742 df; null deviance = 2415.6 on 1743 df; Akaike information criterion [AIC] = 2282.6); logit(decay5%) = $-2.54961 + 0.00454 \times \text{diameter}$ (slope SE = 0.00036, z = 12.74, p < 0.001; residual deviance of 1907.7 on 1742 df; null deviance = 2111.4 on 1743 df; AIC = 1911.7); logit(decay10%) = -3.20951 $+ 0.00497 \times \text{diameter}$ (slope SE = 0.00037, z = 13.51, p < 0.001; residual deviance of 1578.1 on 1742 df; null deviance = 1805.2 on 1743 df; AIC = 1583.1); logit(decay50%) = $-4.63798 + 0.00482 \times \text{diameter}$ (slope SE = 0.00042, z = 11.55, p < 0.001; residual deviance of 751.18 on 1742 df; null deviance = 889.44 on 1743 df; AIC = 755.18). (C) Severity of decay varies greatly across species. Nearly a quarter of species have almost no decay, while 9% have more than half their basal area decayed. Colors of bars indicate ranges of decay severity and are consistent with colors indicating decay severity in panels (B) and (D). (D) Probability of wood decay across 1744 trunks of 172 tree species as a function of species abundance (of stems diameter at standard height [DSH] \geq 20 cm) on the 50-ha plot. Logistic regressions shown for decay thresholds of 2%, 5%, 10%, and 50% of cross-sectional basal area decayed. Regression formulas are logit(decay2%) $= 0.2300 - 0.0467 \times \log_2(abundance)$ (slope SE = 0.02067, z = -2.257, p = 0.024; residual deviance of 2410.5 on 1742 df; null deviance = 2415.6 on 1743 df; AIC = 2414.5); logit(decay5%) = $-0.3471 - 0.0840 \times \log_2(\text{abundance})$ (slope SE = 0.02225, z = -3.778, p < 0.001; residual deviance of 2097.2 on 1742 df; null deviance = 2111.4 on 1743 df; AIC = 2101.2); logit(decay10%) = -0.6876 – $0.0993 \times \log_2(\text{abundance})$ (slope SE = 0.02440, z = -4.068, p < 0.001; residual deviance of 1788.9 on 1742 df; null deviance = 1805.2 on 1743 df; AIC = 1792.9); $\log it(decay50\%) = -1.7480 - 0.1367 \times \log_2(abundance)$ (slope SE = 0.03751, z = -3.644, p < 0.001; residual deviance of 876.64 on 1742 df; null deviance = 889.44 on 1743 df; AIC = 880.64), p < 0.001.

Visual rot and decay associates

We detected visible signs of rot in 81.2% (n = 543) of drilled cores taken from trees in which decay was detected through tomography. Visible rot was more likely to be detected in trunks where tomography indicated greater amounts of decay (Appendix S5: Figure S1A) and

was less likely to be detected in cores from larger trunks, possibly because of the difficulty of drilling to decay areas in the interior of large trees.

Trees with more decay were more likely to have visible fungal structures, as were larger trees (Appendix S5: Figure S1B). However, macroscopic fungal structures on the trunks of trees were not reliable indicators of internal

decay. For instance, of those trees with visible fungal structures, only 39.3% showed decay (at 10% threshold); among trunks without fungal structures, 20.1% showed >10% decay. Similarly, only 11.3% of trunks with >10% decay had visible fungal structures. There was no significant relationship between the severity of decay and visible signs of termite associates, although larger trees were more likely to have termite activity (Appendix S5: Figure S1C). *Azteca* ant associates, while not directly causal to internal decay, were significantly more likely on trees with more severe decay but with no effect of tree size (Appendix S5: Figure S1D).

Tree traits and susceptibility to heart rot

Species with traits associated with fast life histories (faster relative growth rate, lower wood density, greater mortality rates) were more susceptible to heart-rot decay (Appendix S5: Figure S2).

DISCUSSION

Here, we use noninvasive approaches to measure the extent and patterns of internal wood decay in large, living trees in a moist tropical forest. Our results show that hidden wood decay is common in living trees in a tropical forest and accounts for 20% of the total cross-sectional wood area measured and ~1% of aboveground biomass. Half the trees we measured showed decay, with larger trees more likely to be decayed. External inspection of living trees was not a reliable indicator of internal decay, whereas sonic tomography provides a robust, noninvasive method for detecting the presence and cross-sectional extent of decay.

Estimates of carbon storage in forests do not typically account for internal decay of living trees (Chambers et al., 2000), but the prevalence of decay we observed strongly suggests that wood loss to heart rot should be included in such estimates. We calculate an upper limit of the loss of tree biomass to be one-third of the cross-sectional decay area, equivalent to a 1% loss in total aboveground woody biomass (Appendix S2). This volume is less than might be expected based on the prevalence of decay, in part because the most abundant species are the least likely to have severe decay. This estimate could be refined with a better understanding of variation, across fungal and tree species, in the shape of decay columns and in how much biomass is lost in areas with detectable decay.

The tomography results showed that the severity of decay varied greatly among tree species (Figure 1C), and

that, in contrast to the rare-species advantage commonly associated with density-dependent development of diseases of juvenile plants, locally rare species were more likely than common species to have severe internal decay (Figure 1D; Appendix S3). This is consistent with observations that conspecific negative density dependence is stronger in locally rare species than in common species (Comita & Stump, 2020; Xu et al., 2015).

Such a pattern suggests that species-level traits shape innate susceptibility to infection by wood-decay fungi. Although trees have a number of active responses to invasion of woody tissue by fungi (Shigo, 1984), because heart wood is composed of dead tissues, most defenses consist of pre-attack, constitutive components like high wood density, and a range of defensive chemicals, rather than attack-induced defenses (Cornelissen et al., 2012; Kahl et al., 2017). Species vary in the degree to which they invest in these defenses following a wood economics spectrum (Chave et al., 2009; Wright et al., 2010), with fast-growing species having poorly defended, lower density wood and higher mortality rates, in contrast to slower growing species. Indeed, we found that species with faster growth rates, greater mortality rates, and/or lower wood density were more likely to suffer heart rot (Appendix S5). Although covariance among traits means we cannot link individual traits to susceptibility, host life history traits are likely to shape the impact of heart rot.

The life history of wood decay fungi may also contribute to the observation that locally rare species suffer more heart rot than locally common species. Most of the associated polypore fungi have long latent periods (years to decades between infection and reproduction) and movement among trees is dominated by mycelial spread along roots, with only rare wind-borne spore dispersal (Chung et al., 2015; Hansen & Goheen, 2000; Page et al., 2020). Rates of mycelial spread along roots or soil are not well known in tropical systems, but temperate forest fungi spread at rates of 0.1-1 m per year along roots (Bendz-Hellgren et al., 1999; Nelson & Hartman, 1975; Redfern, 1973). On BCI, the median distance to the nearest conspecific neighbor (of stems DSH \geq 20 cm) is 56.5 m (Appendix S4). This means that local spread of decay-causing fungi between conspecific trees is likely a decades-long process, and mature trees are unlikely to exhibit the density-responsive patterns of disease commonly associated with plant pathogens having short latent periods.

There are many reasons why a tree species may be locally rare (Wamelink et al., 2014), but the results of this study suggest that at least some of the rare species (83 of the 171 tree species had ≤10 individuals on the 50-ha plot) may be locally uncommon because they were

ECOLOGY 7 of 9

intrinsically more susceptible to root-, butt-, and heart-rot fungi than other species were species. Similarly, the 10 most abundant tree species (with 199 to 671 individuals on the 50-ha plot) had a much lower mean cross-sectional decay (1.4% decay) compared to the mean of 83 species with ≤10 individuals (9.7% decay). This suggests that broad, innate resistance to decay-causing fungi may be a prerequisite for a large-statured tree species to be common in a tropical forest, and additional studies in different types of tropical forest plots could test the generality of this hypothesis. Direct measurement of variation in resistance traits across species is also an important next step toward understanding the mechanisms driving these patterns.

AUTHOR CONTRIBUTIONS

Research was conceived and designed, and funding acquired, by Stephen P. Hubbell, Travis C. Glenn, Brant C. Faircloth, and Gregory S. Gilbert. Data were collected by Gregory S. Gilbert, Javier O. Ballesteros, César A. Barrios-Rodríguez, Ernesto Bonadies, Marjorie L. Cedeño-Sánchez, Nohely J. Fossatti-Caballero, José Moisés Pérez-Suñiga, and Mariam M. Trejos-Rodríguez. Gregory S. Gilbert conducted the analyses and wrote the first draft. All authors contributed to revising and editing the manuscript.

ACKNOWLEDGMENTS

This project was supported by National Science Foundation grants DEB-1136626 and 1437419 to Stephen P. Hubbell, Brant C. Faircloth, Gregory S. Gilbert, and Travis C. Glenn. We thank S.J. Wright for generously providing updated wood economics spectrum data for BCI trees. The BCI forest dynamics research project was made possible by National Science Foundation grants to Stephen P. Hubbell: DEB grants 0640386, 0425651, 0346488, 0129874, 00753102, 9909347, 9615226, 9405933, 9221033, 9100058, 8906869, 8605042, 8206992, 7922197; support from the Forest Global Earth Observatory (ForestGEO); the Smithsonian Tropical Research Institute (STRI); the John D. and Catherine T. MacArthur Foundation; the Mellon Foundation; the Small World Institute Fund; and numerous private individuals; and through the hard work of over 100 people from 10 countries during the past three decades. The BCI FDP is part of ForestGEO, a global network of large-scale demographic tree plots. The authors thank STRI for logistical support and MiAmbiente for permission to conduct research in the Republic of Panama.

CONFLICT OF INTEREST STATEMENT

The authors declare no conflicts of interest.

DATA AVAILABILITY STATEMENT

Data (Gilbert, 2025) are available on Dryad: https://doi.org/10.5061/dryad.kprr4xhfx.

ORCID

Gregory S. Gilbert https://orcid.org/0000-0002-5195-9903

REFERENCES

- Aguadé, D., R. Poyatos, M. Gómez, J. Oliva, and J. Martínez-Vilalta. 2015. "The Role of Defoliation and Root Rot Pathogen Infection in Driving the Mode of Drought-Related Physiological Decline in Scots Pine (*Pinus sylvestris* L.)." *Tree Physiology* 35: 229–242.
- Augspurger, C. K., and C. K. Kelly. 1984. "Pathogen Mortality of Tropical Tree Seedlings: Experimental Studies of the Effects of Dispersal Distance, Seedling Density, and Light Conditions." *Oecologia* 61: 211–17.
- Balmelli, G., S. Simeto, N. Altier, V. Marroni, and J. J. Diez. 2013. "Long Term Losses Caused by Foliar Diseases on Growth and Survival of *Eucalyptus globulus* in Uruguay." *New Forests* 44: 249–263.
- Barry, K., R. Irianto, E. Santoso, M. Turjaman, E. Widyati, I. Sitepu, and C. Mohammed. 2004. "Incidence of Heartrot in Harvest-Age *Acacia mangium* in Indonesia, Using a Rapid Survey Method." *Forest Ecology and Management* 190: 273–280.
- Basham, J. 1973. "Heart Rot of Black Spruce in Ontario. I. Stem Rot, Hidden Rot, and Management Considerations." *Canadian Journal of Forest Research* 3: 95–104.
- Bendz-Hellgren, M., P.-O. Brandtberg, M. Johansson, G. Swedjemark, and J. Stenlid. 1999. "Growth Rate of *Heterobasidion annosum* in *Picea abies* Established on Forest Land and Arable Land." *Scandinavian Journal of Forest Research* 14: 402–7.
- Blundo, C., J. Carilla, R. Grau, A. Malizia, L. Malizia, O. Osinaga-Acosta, M. Bird, et al. 2021. "Taking the Pulse of Earth's Tropical Forests Using Networks of Highly Distributed Plots." *Biological Conservation* 260: 108849.
- Boyle, B., N. Hopkins, Z. Lu, J. A. Raygoza Garay, D. Mozzherin, T. Rees, N. Matasci, et al. 2013. "The Taxonomic Name Resolution Service: An Online Tool for Automated Standardization of Plant Names." *BMC Bioinformatics* 14: 1–15.
- Bruck, R. 1989. "Survey of Diseases and Insects of Fraser Fir and Red Spruce in the Southern Appalachian Mountains." European Journal of Forest Pathology 19: 389–398.
- Cabon, A., S. A. Kannenberg, A. Arain, F. Babst, D. Baldocchi, S. Belmecheri, N. Delpierre, et al. 2022. "Cross-Biome Synthesis of Source Versus Sink Limits to Tree Growth." Science 376: 758–761.
- Chambers, J. Q., N. Higuchi, J. P. Schimel, L. V. Ferreira, and J. M. Melack. 2000. "Decomposition and Carbon Cycling of Dead Trees in Tropical Forests of the Central Amazon." *Oecologia* 122: 380–88.
- Chave, J., C. Andalo, S. Brown, M. A. Cairns, J. Q. Chambers, D. Eamus, H. Fölster, et al. 2005. "Tree Allometry and Improved Estimation of Carbon Stocks and Balance in Tropical Forests." *Oecologia* 145: 87–99.

Chave, J., D. Coomes, S. Jansen, S. L. Lewis, N. G. Swenson, and A. E. Zanne. 2009. "Towards a Worldwide Wood Economics Spectrum." *Ecology Letters* 12: 351–366.

- Chung, C.-L., S.-Y. Huang, Y.-C. Huang, S.-S. Tzean, P.-J. Ann, J.-N. Tsai, C.-C. Yang, et al. 2015. "The Genetic Structure of *Phellinus noxius* and Dissemination Pattern of Brown Root Rot Disease in Taiwan." *PLoS One* 10: e0139445.
- Comita, L. S., and S. M. Stump. 2020. "Natural Enemies and the Maintenance of Tropical Tree Diversity: Recent Insights and Implications for the Future of Biodiversity in a Changing World." *Annals of the Missouri Botanical Garden* 105: 377–392.
- Condit, R., R. Perez, S. Aguilar, S. Lao, R. Foster, and S. P. Hubbell. 2019a. "BCI 50-ha Plot Taxonomy, 2019 Version." Dryad. https://doi.org/10.15146/R3FH61.
- Condit, R., R. Perez, S. Aguilar, S. Lao, R. Foster, and S. P. Hubbell. 2019b. "Complete Data from the Barro Colorado 50-ha Plot: 423617 Trees, 35 Years, 2019 Version." Dryad. https://doi.org/10.15146/5xcp-0d46.
- Cornelissen, J. H., U. Sass-Klaassen, L. Poorter, K. van Geffen, R. S. van Logtestijn, J. van Hal, L. Goudzwaard, et al. 2012. "Controls on Coarse Wood Decay in Temperate Tree Species: Birth of the LOGLIFE Experiment." Ambio 41: 231–245.
- Davies, S. J., I. Abiem, K. A. Salim, S. Aguilar, D. Allen, A. Alonso, K. Anderson-Teixeira, et al. 2021. "ForestGEO: Understanding Forest Diversity and Dynamics through a Global Observatory Network." *Biological Conservation* 253: 108907.
- Delaye, L., G. Garcia-Guzman, and M. Heil. 2013. "Endophytes Versus Biotrophic and Necrotrophic Pathogens-Are Fungal Lifestyles Evolutionarily Stable Traits?" Fungal Diversity 60: 125–135.
- Dobbertin, M., A. Baltensweiler, and D. Rigling. 2001. "Tree Mortality in an Unmanaged Mountain Pine (*Pinus mugo* var. *uncinata*) Stand in the Swiss National Park Impacted by Root Rot Fungi." *Forest Ecology and Management* 145: 79–89.
- Fukasawa, Y. 2021. "Ecological Impacts of Fungal Wood Decay Types: A Review of Current Knowledge and Future Research Directions." *Ecological Research* 36: 910–931.
- Gilbert, G. 2025. "Data For: Hidden Decay of Live Trees in a Tropical Rain Forest." Dataset. Dryad. https://doi.org/10.5061/ dryad.kprr4xhfx.
- Gilbert, G. S., J. O. Ballesteros, C. A. Barrios-Rodriguez, E. F. Bonadies, M. L. Cedeño-Sánchez, N. J. Fossatti-Caballero, M. M. Trejos-Rodríguez, et al. 2016. "Use of Sonic Tomography to Detect and Quantify Wood Decay in Living Trees." Applications in Plant Sciences 4: 1600060.
- Gonzalez-Akre, E., C. Piponiot, M. Lepore, V. Herrmann, J. A. Lutz, J. L. Baltzer, C. Dick, et al. 2021. "Allodb: An R Package for Biomass Estimation at Globally Distributed Extratropical Forest Plots." Methods in Ecology and Evolution 13: 330–38.
- Hansen, E. M., and E. M. Goheen. 2000. "Phellinus weirii and Other Native Root Pathogens as Determinants of Forest Structure and Process in Western North America." Annual Review of Phytopathology 38: 515–539.
- Hellgren, M. B., and J. Stenlid. 1995. "Long-Term Reduction in the Diameter Growth of Butt Rot Affected Norway Spruce, *Picea abies." Forest Ecology and Management* 74: 239–243.

- Hubbell, S. P., R. B. Foster, S. T. O'Brien, K. E. Harms, R. Condit, B. Wechsler, S. J. Wright, et al. 1999. "Light-Gap Disturbances, Recruitment Limitation, and Tree Diversity in a Neotropical Forest." *Science* 283: 554–57.
- Johnson, D. J., W. T. Beaulieu, J. D. Bever, and K. Clay. 2012. "Conspecific Negative Density Dependence and Forest Diversity." *Science* 336: 904–7.
- Kahl, T., T. Arnstadt, K. Baber, C. Bässler, J. Bauhus, W. Borken, F. Buscot, et al. 2017. "Wood Decay Rates of 13 Temperate Tree Species in Relation to Wood Properties, Enzyme Activities and Organismic Diversities." Forest Ecology and Management 391: 86–95.
- Kodrík, J., and M. Kodrík. 2002. "Root Biomass of Beech as a Factor Influencing the Wind Tree Stability." *Journal of Forest Science* 48: 549–564.
- Kõrkjas, M., L. Remm, and A. Lõhmus. 2021. "Development Rates and Persistence of the Microhabitats Initiated by Disease and Injuries in Live Trees: A Review." Forest Ecology and Management 482: 118833.
- Lutz, J. A., T. J. Furniss, D. J. Johnson, S. J. Davies, D. Allen, A. Alonso, K. J. Anderson-Teixeira, et al. 2018. "Global Importance of Large-Diameter Trees." Global Ecology and Biogeography 27: 849–864.
- Martin, A. R., G. M. Domke, M. Doraisami, and S. C. Thomas. 2021. "Carbon Fractions in the World's Dead Wood." *Nature Communications* 12: 889.
- Nelson, E., and T. Hartman. 1975. "Estimating Spread of Poria weirii in a High-Elevation, Mixed Conifer Stand." Journal of Forestry 73: 141–42.
- Nogueira, E. M., B. W. Nelson, and P. M. Fearnside. 2006. "Volume and Biomass of Trees in Central Amazonia: Influence of Irregularly Shaped and Hollow Trunks." *Forest Ecology and Management* 227: 14–21.
- Page, D. E., M. Glen, D. Puspitasari, I. Prihatini, A. Gafur, and C. L. Mohammed. 2020. "Acacia Plantations in Indonesia Facilitate Clonal Spread of the Root Pathogen Ganoderma philippii." Plant Pathology 69: 685–697.
- PiCUS. 2015. *PiCUS TreeTronic Manual Q72.x.* Hong Kong: Promat (HK) Limited.
- Redfern, D. 1973. "Growth and Behaviour of Armillaria mellea Rhizomorphs in Soil." Transactions of the British Mycological Society 61: 569.
- Rojo, M. J., and J. Paquit. 2018. "Incidence of Heart Rot in a University Owned Plantation Forest: Implication on Forest Management." *Journal of Biodiversity and Environmental Sciences* 13: 146–151.
- Russell, M. B., S. Fraver, T. Aakala, J. H. Gove, C. W. Woodall, A. W. D'Amato, and M. J. Ducey. 2015. "Quantifying Carbon Stores and Decomposition in Dead Wood: A Review." Forest Ecology and Management 350: 107–128.
- Shigo, A. L. 1984. "Compartmentalization: A Conceptual Framework for Understanding how Trees Grow and Defend themselves." *Annual Review of Phytopathology* 22: 189–214.
- Sudin, M., S. S. Lee, and A. H. Harun. 1992. "A Survey of Heart Rot in some Plantations of *Acacia mangium* in Sabah." *Journal of Tropical Forest Science* 6: 37–47.
- Sundararaj, R., P. Swetha, S. Mondal, M. Kantha Reddy, R. Raja Rishi, and N. Mamatha. 2023. "Incidence and Effect of Heart Rot in Marayur Sandalwood (*Santalum album L.*) Reserve,

19399170, 2025, 9, Downloaded from https://esajo elibrary.wiley.com/doi/10.1002/ecy.70208 by Louisiana State University, Wiley Online Library on [24/11/2025]. See the Term

ECOLOGY 9 of 9

Kerala, and its Natural Durability against Fungi." Forest Science 69: 133–142.

- Wamelink, G. W., P. W. Goedhart, and J. Y. Frissel. 2014. "Why Some Plant Species Are Rare." *PLoS One* 9: e102674.
- Worrall, J. J., T. D. Lee, and T. C. Harrington. 2005. "Forest Dynamics and Agents that Initiate and Expand Canopy Gaps in *Picea–Abies* Forests of Crawford Notch, New Hampshire, USA." *Journal of Ecology* 93: 178–190.
- Wright, S. J., K. Kitajima, N. J. Kraft, P. B. Reich, I. J. Wright, D. E. Bunker, R. Condit, et al. 2010. "Functional Traits and the Growth–Mortality Trade-Off in Tropical Trees." *Ecology* 91: 3664–74.
- Xu, M., Y. Wang, and S. Yu. 2015. "Conspecific Negative Density Dependence Decreases with Increasing Species Abundance." *Ecosphere* 6: 1–11.

SUPPORTING INFORMATION

Additional supporting information can be found online in the Supporting Information section at the end of this article.

How to cite this article: Gilbert, Gregory S., Brant C. Faircloth, Travis C. Glenn, Javier O. Ballesteros, César A. Barrios-Rodríguez, Ernesto Bonadies, Marjorie L. Cedeño-Sánchez, et al. 2025. "Hidden Decay of Live Trees in a Tropical Rain Forest." *Ecology* 106(9): e70208. https://doi.org/10.1002/ecy.70208